Response of a reinforced concrete structure to explosive loads

Androniki-Anna Doulgeroglou[a,c,*], Panagiotis Kotronis[a,*], Giulio Sciarra[a,*], Abdul-Hamid Soubra[b,], Yves Jaboin[c,***]**

a. École Centrale de Nantes, Université de Nantes, CNRS
Institut de Recherche en Génie Civil et Mécanique (GeM), UMR 6183
1 rue de la Noë, BP 92101, 44321, Nantes, cedex 3, France
b. Université de Nantes, CNRS
Institut de Recherche en Génie Civil et Mécanique (GeM), UMR 6183
Bd de l'Université, 44600 Saint-Nazaire, France
c. Groupe NOX, Arbor Jovis, 3 Boulevard du Zenith, 44800 Saint Herblain, France
* {androniki-anna.doulgeroglou, panagiotis.kotronis, giulio.sciarra}@ec-nantes.fr
** abed.soubra@univ-nantes.fr
*** y.jaboin@groupe-nox.com

Résumé :

L'objectif de cet article est l'étude numérique du comportement d'un portique en béton armé jusqu'à la ruine, en considérant des charges explosives. Pour cela, une poutre Timoshenko avec une discontinuité intégrée au champ de la rotation, récemment développée par Bitar et al [4] sera adoptée. Dans le cadre du code matlab des éléments finis développé par Bonnet et Frangi [5], des éléments poutres intégrant de fortes discontinuités ont été implémentés [4], de sorte que le comportement adoucissant et l'ouverture de la fissure sont décrits, en utilisant une loi cohésive qui permet de capturer la réduction de résistance et la dissipation d'énergie. Dans ce travail, afin de représenter la charge cyclique, nous étendrons la loi cohésive et la loi de comportement généralisée liant le moment de flexion avec la rotation, représentative d'une section en béton armé. La charge sur la structure par des explosions est décrite par une dépendance appropriée de la pression de souffle en fonction du temps. Une estimation de cette distribution de pression est obtenue en utilisant la méthodologie développée par l'US Army Corps of Engineers [18]. Les effets de l'interaction fluide-structure ne sont pas pris en compte. L'efficacité du modèle proposé sera verifiée par des comparaisons avec des simulations du code des éléments finis Cast3M.

Abstract :

The purpose of this paper is to numerically study the behavior of a reinforced concrete frame up to failure considering explosive loads. For this, a recently developed generalized Timoshenko beam with embedded rotation discontinuity [4] will be adopted. Within the framework of the finite element matlab code developed by Bonnet and Frangi [5], beam elements that incorporate strong discontinuities were implemented [4] so that the softening behavior and the crack opening are described, using a cohesive law that allows for capturing strength reduction and energy release. In this work, in order to represent cyclic loading, we will extend the cohesive law and the generalized constitutive law linking the bending

moment with the rotation, representative of a reinforced concrete section. Loading on the structure due to explosions is described by a suitable blast pressure dependency on time. An estimation of this pressure distribution is obtained using the methodology developed by the U.S. Army Corps of Engineers [18]. The effects of the fluid structure interaction are not considered. The efficiency of the proposed model will be verified by comparisons with simulations from the finite element code Cast3M.

Keywords : Explosions, Timoshenko beam, discontinuities, cohesive law, non-linear analysis.

1 Introduction

An explosion is a phenomenon during which a sudden release of energy takes place. At the location of the explosion, energy is locally accumulated and then by different forms, such as blast waves, it is suddenly dissipated. The study of the effects of an exterior explosion on a structure is a procedure of high complexity. This complexity may be explained by many factors which are related to the explosive load calculation, the non-linear behavior of the structure and the lack of guidelines in the Eurocode. Research on this subject is mainly conducted by the military forces and the resulting experimental data are not always accessible to the public. However, publications with free access have been made by the US Department of Defense [18], concerning the blast load calculation and the evaluation of the response of structural elements under blast loading.

2 Explosion and blast wave phenomena

In this section a brief introduction to the basics of explosions and loads from blast waves that are created will be given. The material is based on [1], [10], [11], [12] and [18]. The term explosion covers phenomena for which physicochemical processes may be different. According to their nature explosions are divided into physical, nuclear or chemical. A chemical detonating explosion can be confined or unconfined. The unconfined explosions, which occur in free space, are divided into free-air bursts, air bursts and surface bursts (see Figure 1 (a), (b) and (c) respectively).

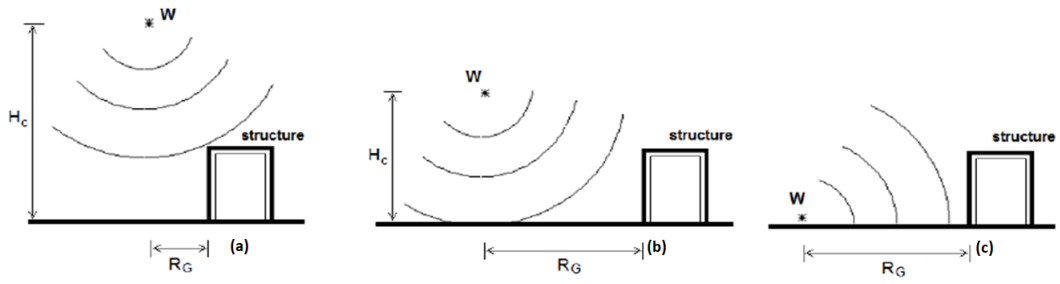

Figure 1: Unconfined explosions in free air space [18]

Free-air bursts create spherical waves (Fig. 1 (a), (b)) and surface bursts create hemispherical waves (Fig. 1 (c)). The magnitude and the distribution of the blast loads are function of (i) the explosive properties, such as the type of explosive material, (ii) the location of detonation with respect to the structure and (iii) the magnitude and the reinforcement of the pressure by its interaction with the ground or the structure itself.

When a condensed high explosive is initiated, firstly the explosion reaction generates hot gases which expand violently. Then, the surrounding air is forced out of the volume it occupies and a layer of compressed air - the blast wave - forms in front of these gases containing most of energy released by the explosion. The blast wave or shock front is characterized by an almost instantaneous rise from ambient pressure to a peak incident overpressure (point B in Figure 2).

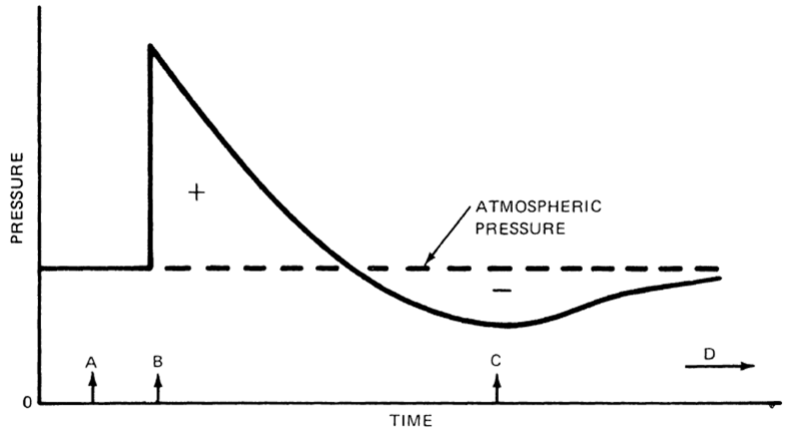

Figure 2: Blast wave pressures plotted against time [12]

As the wave expands, it decays in strength, lengthens in duration and decreases in velocity (Figure 3). Gas molecules behind the front move at lower flow/particle velocities.These particle velocities are associated with the dynamic pressures which correspond to the pressures formed by the winds produced by the passage of the shock front. The pressure of the explosively formed gases falls to atmospheric pressure and the pressure of the compressed air at the blast wavefront also falls with increasing distance.

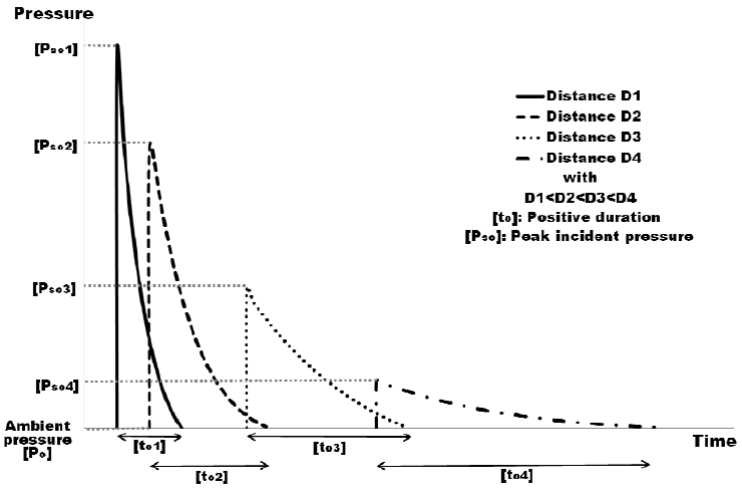

Figure 3: Influence of distance on the blast positive pressure phase [11]

As the explosive gases continue to expand, they cool and their pressure falls a little below atmospheric pressure. A region of underpressure (called negative phase) where pressure is below atmospheric is thus induced. Eventually the situation returns to equilibrium as the air and gases pushed away from the source

return. In this study, both positive and negative phases will be taken into account for the evaluation of the overall motion of the structure. It should be noted here that the structure motions are caused by the shock loads. The latters are divided into ground and air shocks. This study ignores the effect of the shock transmitted by the ground to the structure.

2.1 Calculation of the blast wave parameters

The blast wave parameters are established through the application of scaling laws and the TNT equivalency. The scaling law for explosions is based on fundamentals of geometrical similarity and conservation of momentum and is used to find descriptions for explosions which are not defined quantitatively through experimental studies. The TNT equivalency is used to equate a particular explosion source to a mass of TNT by considering the energy contained within the source. TNT is widely accepted as the basis for comparison with other condensed high explosives materials. In order to take into consideration specific uncertainties which can lead to an overestimation of a structure's capacity under an explosive load, such as unexpected shock wave reflections, construction methods or quality of construction materials, it is recommended to apply a 20% increase of the equivalent TNT mass. The calculation of the blast wave parameters is then done with this increased value of the charge, the effective charge weight.

The methodology for the calculation of the pressure-time dependent curves is well described in UFC [18] and is based on experimental results, semi-empirical relations and extrapolation laws. The principle of this method relies on the approximation of this curve, which is obtained by the triangularisation of the real curve (Figure 4).

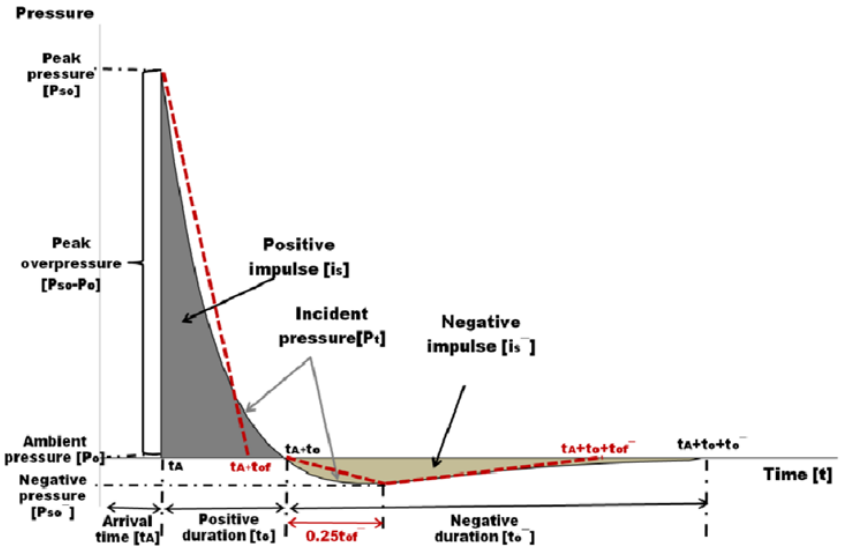

Figure 4: Substitution of actual incident pressure curve by triangular pulses and definition of relevant fictious times [11]

A direct blast wave firstly impinges the front face of the structure. Then, as the wave propagates, it surrounds the structure and as a result pressures are loading the roof, the sides and the rear surface. Thus, a pressure-time history curve is constructed for every surface of the structure. In Figure 5 a typical pressure time dependent curve on the front face of a structure is presented. The peak pressure corresponds to the reflected pressure and decreases until the pressure gets equal to the pressure of the surrounding air.

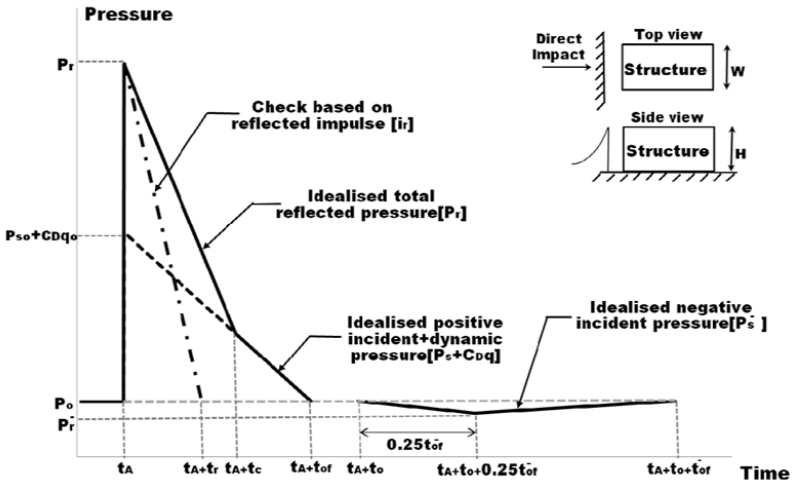

Figure 5: Triangular assumption of pressure time history on the front face of a structure [11]

3 Material behavior

Explosive loads produce very high strain rates in the range of 10^2 - 10^4 s^{-1}. These strain rates can change the mechanical properties of the structures loaded by blast pressures. A structural element subjected to a blast loading exhibits a higher strength than a similar element subjected to a static loading. The rapid rates of strain during dynamic loads result in the increase in strength of concrete and reinforcing steel materials. The stresses that can be sustained by concrete during fast loading may be magnified up to 4 times in compression and up to 6 times in tension with reference to the static ones. Figures 6 and 7 present some experimental results of the litterature on the effect of the strain rate on the tensile and compressive strength of the concrete respectively.

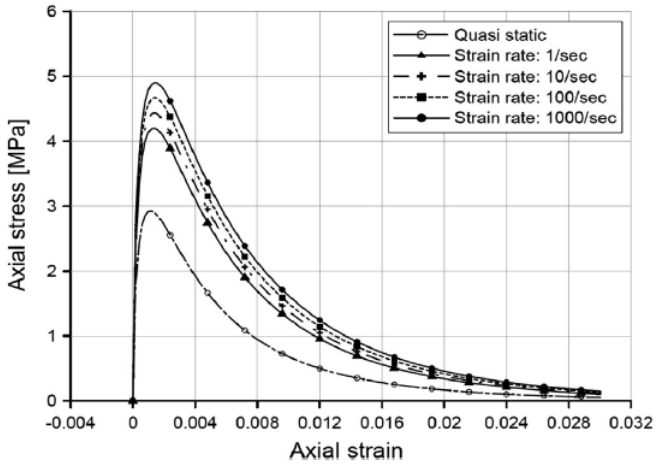

Figure 6: Strain rate dependent tensile stress versus strain [16]

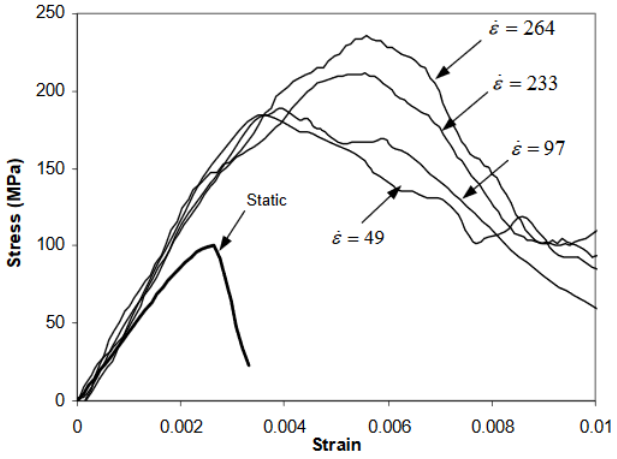

Figure 7: Strain rate dependent compressive stress versus strain [15]

Reinforcing steel presents almost double lower yield strength, as it was shown by experiments conducted by Dowling and Harding [8]. Furthermore, under higher strain rates, the ultimate tensile strength of the steel can be increased by 50%, while the ultimate tensile strain of the steel decreases.

4 Response of the structure

In the literature, there can be found a number of works that deal with the effects of blast loads on reinforced concrete structures. In UFC [18] there is a proposed simplified methodology for the evaluation of the structural response considering explosive loads, by the calculation of the final states. This methodology is based on the idealization of the structure as a single degree of freedom system and relies on considering the energies of the real structure and the equivalent system and equating them. To convert the real system to the equivalent one, transformation factors are used. This method adopts the assumptions that the deflected shape is known and that one mode predominates in the response to short duration loads. More information can be found in [18] and [2]. We note here that damping is usually negligible in blast design, as it has very little effect on the first peak of response which is usually the only cycle of response.

Other approaches of dynamic analysis involve the use of finite element codes. For example, Chen et al [7] analysed with the LS-DYNA finite element code prestressed reinforced concrete beams with different prestress, concrete strength and blast loading. In that study, 8-node solid elements for modelling the concrete and 2-node beam elements for the steel were used. The constitutive model for the concrete considered strain-rate effects, plasticity and damage softening after failure, while for the steel the corresponding model considered isotropic and kinematic hardening plasticity. Li et al [13] simulated reinforced concrete columns with the hydrocode of LS-DYNA, by using the same types of elements as in [7], in order to study the spalling damage caused by blast and impact loading. The constitutive model for the concrete was a plasticity-based-model, while for the steel an isotropic and kinematic hardening plasticity model was chosen. The same damage mechanism was studied by Yan et al [20] for reinforced concrete beams, by using the same type of finite elements and constitutive models for concrete and steel materials. Luccioni et al [14] analysed the collapse of an exising building with hydrocodes in AUTODYN and compared their results with photos. An approximate homogenised elastoplastic material model for reinforced concrete elements was used. Other finite element codes are also used for the

assessment of a structure which is subjected to blast loads. Draganić et al [9] used the finite element code SAP2000 to study a fictive structure under blast loading. They modelled girders and columns with beam elements and slabs and walls with shell elements. The chosen models for concrete and steel were of Takeda hysterisis type and Kinematic hysterisis type respectively. The authors showed that with conventional finite element codes and the introduction of a load scenario in the program as pressure-time history, preliminary results for the response of the building can be obtained.

5 Numerical study of a reinforced concrete structure under blast loads

In order to study the response of a reinforced concrete structure, subjected to explosive loads a generalized Timoshenko beam element following the Full-Cubic-Quadratic formulation (FCQ) by Caillerie et al [6] is used. A blast load scenario is employed. The purpose of this research is to study the two-story frame, experimentally studied in the scale of one by Vecchio et al [19]. The geometry of the frame and the sections corresponding to the beams and the columns are presented in Figure 8. The effects of soil-structure interaction are not taken into account in this study.

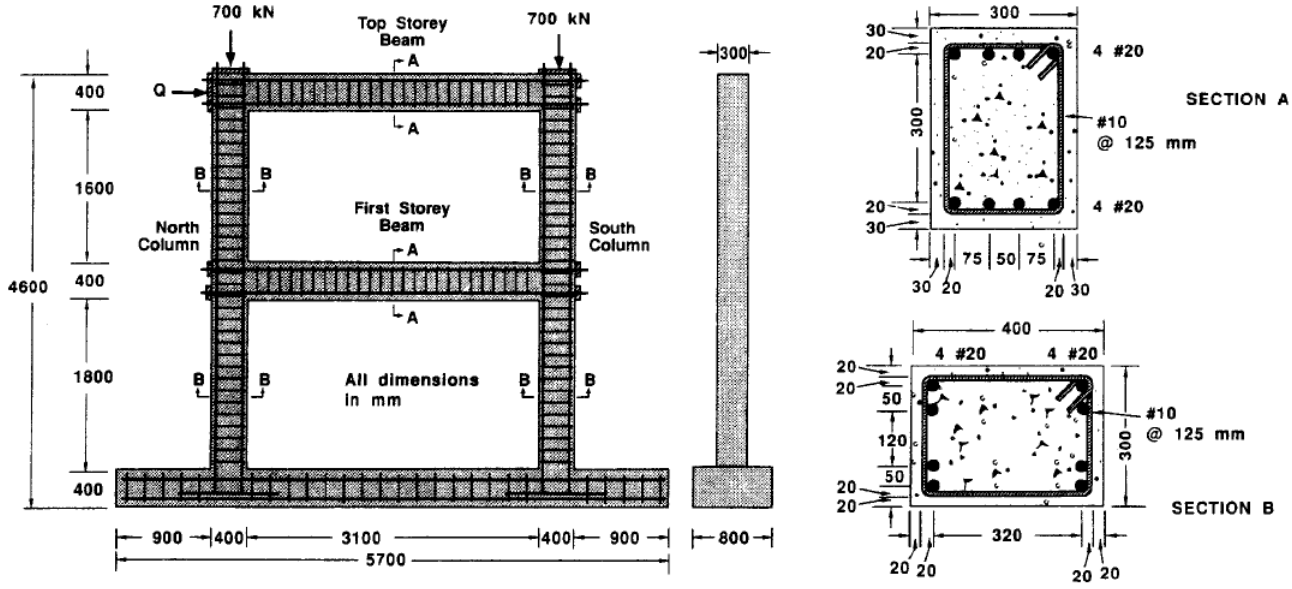

Figure 8: Geometry of the frame and reinforcement details [19]

According to the blast scenario, blast pressures verus time are calculated for the front face, the roof and the rear face. Preliminary calculations took place, by considering one beam of this structure. In our study, we consider a beam of length $3.5m$ fixed at one side. The beam of the second floor (roof) is studied and is discretised by four beam elements, as it is shown in Figure 9. Its geometry and properties were given in [19] (Figure 8). The applied load is the one that was calculated for the roof of the frame. The results presented in this paper will be enriched by considering the whole structure at the sequence of this work.

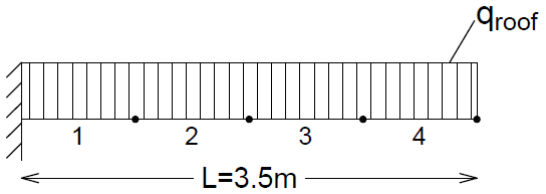

Figure 9: Beam model discretised by 4 elements

5.1 Finite element model

A beam element is a simplified model at the global scale. At this scale, in order to reduce the number of degrees of freedom and to simplify the global equilibrium equations certain kinematic assumptions are adopted. The Timoshenko beam theory is adopted in order to account for the influence of shear strains and stresses. The section of this element is considered homogeneous and stress resultant models are used to describe its behavior.

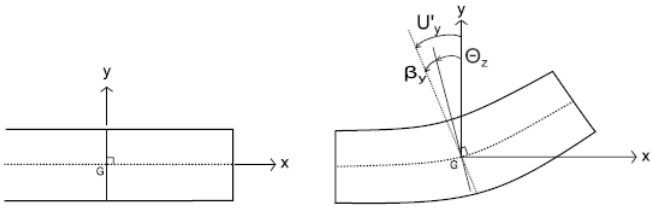

Figure 10: Kinematics of Timoshenko beam [3]

FCQ is a displacement-based Timoshenko beam finite element, that uses shape functions of order one for the axial displacement, three for the transverse displacement and two for the rotation. This formulation possesses an additional internal node. The advantage of this formulation is that one element gives the exact displacements at the nodes for any loading under linear elasticity. More information can be found in [6] and [3]. Hereafter only a brief description of the mathematical formulation is presented. Considering the 2D case of a beam with a length L, a cross - section $S(x)$ and its middle axis oriented towards the x direction, the generalized displacement vector $U(x)$ of the cross section $S(x)$ takes the following form:

$$\mathbf{U}(x) = \begin{bmatrix} U_x(x) & U_y(x) & \Theta_z(x) \end{bmatrix}^\top \tag{1}$$

with $Ux(x)$, $Vy(x)$ and $\Theta_z(x)$ being the longitudinal displacement, the transverse displacement and

the rotation of the section respectively. The generalized displacement field for the FCQ formulation is:

$$\begin{bmatrix} U_x \\ U_y \\ \Theta_z \end{bmatrix} = \begin{bmatrix} N_1 & 0 & 0 & 0 & 0 & 0 & N_7 & 0 & 0 \\ 0 & N_{11} & 0 & N_{13} & 0 & N_{15} & 0 & N_{17} & 0 \\ 0 & 0 & N_{21} & 0 & N_{23} & 0 & 0 & 0 & N_{27} \end{bmatrix} \begin{bmatrix} U_{xi} \\ U_{yi} \\ \Theta_{zi} \\ \Delta U^1_{yk} \\ \Delta\Theta_k \\ \Delta U^2_{yk} \\ U_{xj} \\ U_{yj} \\ \Theta_{zj} \end{bmatrix}, \tag{2}$$

with ΔU^1_{yk}, $\Delta\Theta_k$ and ΔU^2_{yk} being the degrees of freedom of the internal node k. The generalized strain field for the FCQ formulation is derived as:

$$\begin{bmatrix} U'_x \\ \beta_y \\ \Theta'_z \end{bmatrix} = \begin{bmatrix} N'_1 & 0 & 0 & 0 & 0 & 0 & N'_7 & 0 & 0 \\ 0 & N'_{11} & -N_{21} & N'_{13} & -N_{23} & N'_{15} & 0 & N'_{17} & -N'_{27} \\ 0 & 0 & N'_{21} & 0 & N'_{23} & 0 & 0 & 0 & N'_{27} \end{bmatrix} \begin{bmatrix} U_{xi} \\ U_{yi} \\ \Theta_{zi} \\ \Delta U^1_{yk} \\ \Delta\Theta_k \\ \Delta U^2_{yk} \\ U_{xj} \\ U_{yj} \\ \Theta_{zj} \end{bmatrix}. \tag{3}$$

5.2 Blast loading curves

A blast loading scenario was adopted by considering a surface burst of $200kgr$ of TNT explosive at a distance of $30m$ from the stucture. The pressure-time curves were obtained by the application of the methodology in UFC, for the front face, the roof and the rear face respectiveley, as shown in Figure 11.

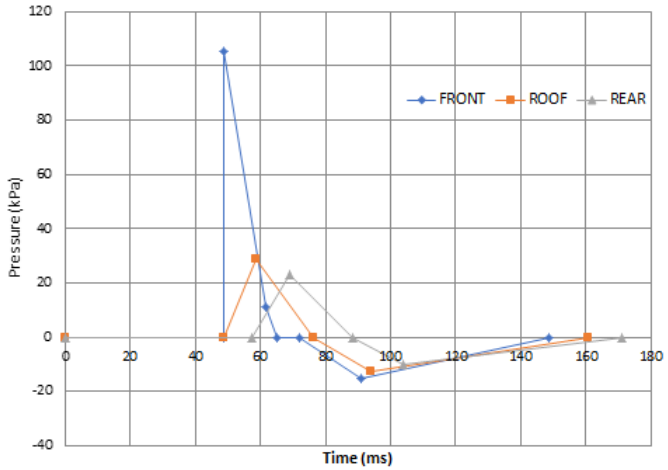

Figure 11: Pressure-time curves for each face of the building

5.3 Constitutive models and material parameters

Two linear elastic stress-resultant models are used to describe the axial and the shear behavior of the section of the beam element

$$F_x = ES\varepsilon_x \qquad F_y = kGS\beta_y \tag{4}$$

with $ES = 3432000$kN and $kGS = 1000000$kN. The moment-curvature model used is a non-linear one. In Figure 12 the continuous (left) and the cohesive model (right) are presented, where M_c is the bending moment at the first crack of the concrete, M_y is the value at which steel enters in plasticity and M_u is the ultimate moment of the section. Additionally, EI is the elastic bending modulus, K_1 the first hardening modulus, K_2 the second hardening modulus and $\bar{\bar{K}}$ the softening modulus of the generalised cohesive model. This model, was developped by [17] for the study of the response of a reinforced concrete beam under static monotonic loading up to failure. For this reason, at this step of this work, we used only the continuous trilinear model (within the plasticity framework), as the coupling of the latter with the cohesive model of the Figure 12 does not correspond to cyclic conditions of loading. One of the most important perspectives of this work is the construction of 3D interaction diagrams for reinforced concrete sections that take into account the cyclic nature of the loading. More specifically, failure surfaces that account for the coupling of the components of moment, shear and axial generalised forces will be constructed and will be used with a cohesive model (as a first step only at the rotation field and without coupling the other components) that takes into account the cyclic loading and is able to describe the reinforced concrete softening behavior under dynamic loads.

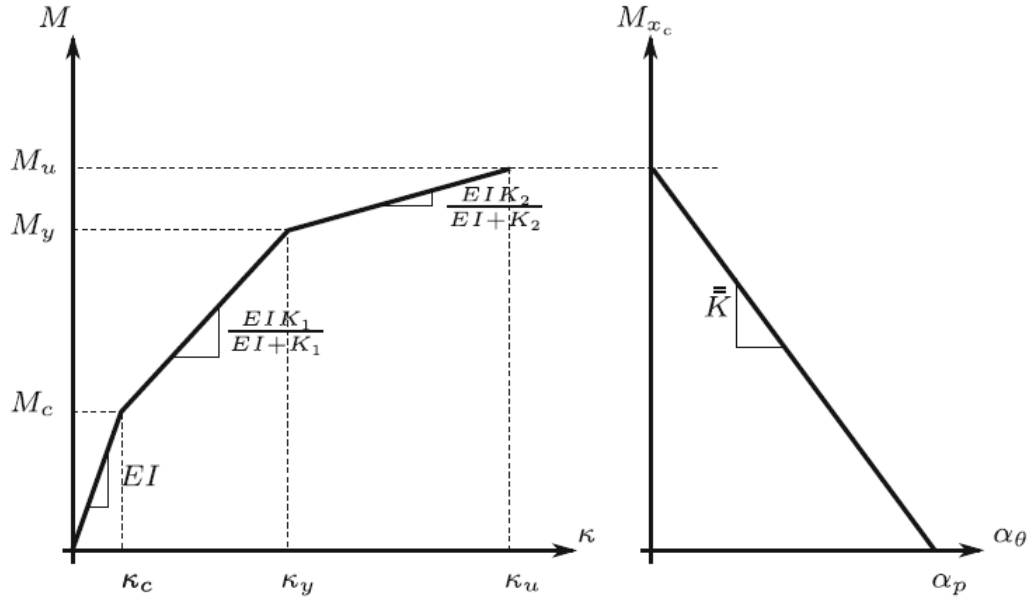

Figure 12: Stress-resultant model: Moment-curvature relation [17]

The parameters of this model are taken from [4] as M_c = $30kN.m$, M_y = $150kN.m$, M_u = $185kN.m$, EI = $45760kN.m^2$, K_1= $11190kN.m^2$, K_2= $137kN.m^2$ and $\bar{\bar{K}}$=$-1310kN.m$.

In order to consider the increase of the strength of the concrete and the steel during fast loading, as a first step we consider two Dynamic Increase Factors (DIF) for the concrete and the steel equal to 1.25 and 1.05, according to [18] and we multiply the M_c and M_y by these factors respectively. This is a first

approximation that considers the strain rate effect in a simplified way. As the point (κ_c,M_c) corresponds to the initial cracking of the concrete M_c is multiplied by a constant DIF for the concrete and for the point (κ_y,M_y) which corresponds to the yielding point of the reinforcing steel M_y is multiplied by a constant DIF proposed for steel material.

5.4 Preliminary results

In this section we present the first preliminary results of our simulations, concerning the beam of the Figure 9, conducted with the Matlab finite element code and the original FCQ formulation without embedded discontinuities. A static cyclic type of analysis (implicit scheme) took place and for the pseudo-time discretisation 125 steps were chosen. This type of analysis neglects the inertia effects, which are very important for the study of structures loaded by explosive loads and damping effects, which are usually negligible in blast design. The consideration of the term of inertial forces is one of the main perspectives of this work. In order to obtain a first comparison with another numerical model, a second finite element model was elaborated in the finite element code Cast3M, using 2D Timoshenko beam elements, the Takeda bending model and by adopting similar parameters. In the following figures both results from the two codes are presented. Figures 13 and 14 show the evolution of the bending moment and the transversal reaction versus time.

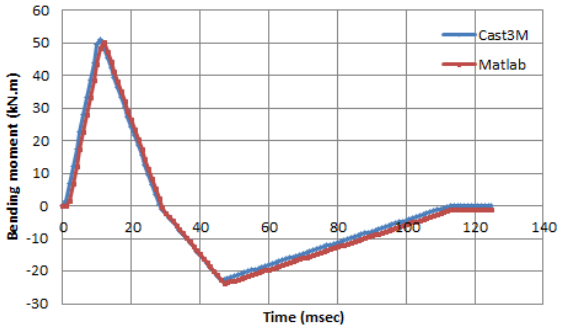

Figure 13: Bending moment - Time

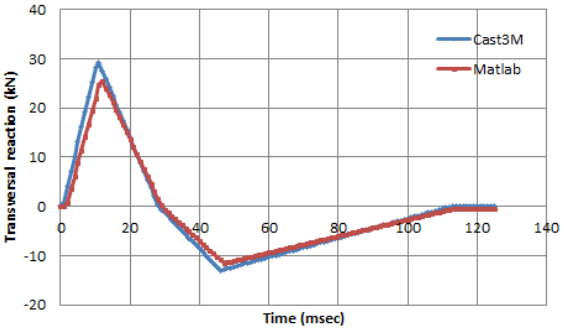

Figure 14: Transversal reaction - Time

The bending moment at the fixed point versus the rotation of the free edge is presented in Figure 15 and the transversal reaction at the fixed point versus the transversal displacement of the free edge is presented in Figure 16 .

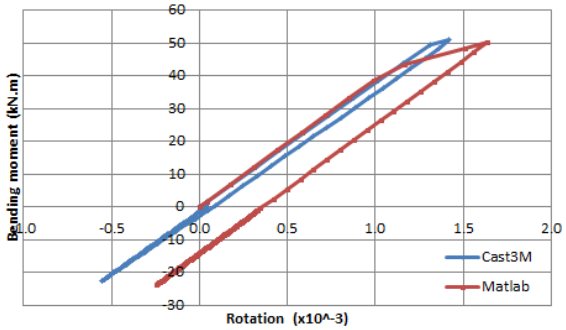

Figure 15: Bending moment - Rotation

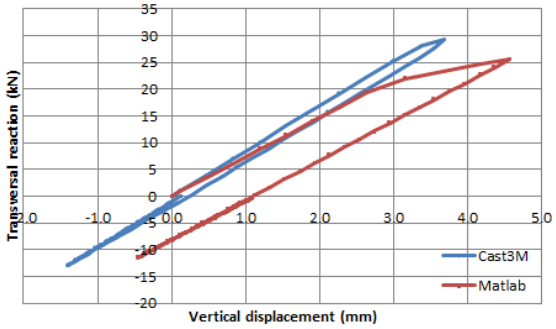

Figure 16: Transversal reaction - Vertical dsiplacement

During the positive loading phase, the two models represent quite similarily the bending behavior of the beam, while during the positive unloading phase there are differences that are related to the callibration of the Takeda model in Cast3M. For both models, the negative phase of the explosion is completely inside the elastic area.

6 Conclusions and perspectives

The numerical model is using the original version of the FCQ formulation, described above, which does not take into account the discontinuities. A generalized constitutive law is used to describe the axial, the shear and the bending behavior. For the axial and the shear behavior a linear relation is chosen, while for the bending behavior a general non-linear relation is chosen accounting for the cyclic nature of the loading within the plasticity framework. A member of the structure was studied individually, by the statical application of the blast loads.

Further research will be conducted so that the generalised constitutive law for the moment-rotation is obtained for fast loading for representative sections of the frame, using the multi-scale approach. More specifically, suitable constitutive laws that represent the behavior of the two materials (concrete and steel) under fast dynamic loads will be chosen and will be implemented in a Timoshenko multi-fiber beam in the finite element code Cast3M. Thus, a general relation that links the bending moment to the rotation of a section can be obtained. The moment - rotation relations will be calibrated to fit experimental data and they will be introduced to the Matlab finite element code that uses the enriched FCQ formulation with strong discontinuities. We show characteristically in Figure 17 the bending behavior of a fixed beam of unit length subjected to cyclic rotation at its free edge following the FCQ formulation without discontinuity (isostropic hardening) and with embedded discontinuity (softening behavior). Simulations will take place for the whole structure by applying the explosive loads to all the faces of the structure.

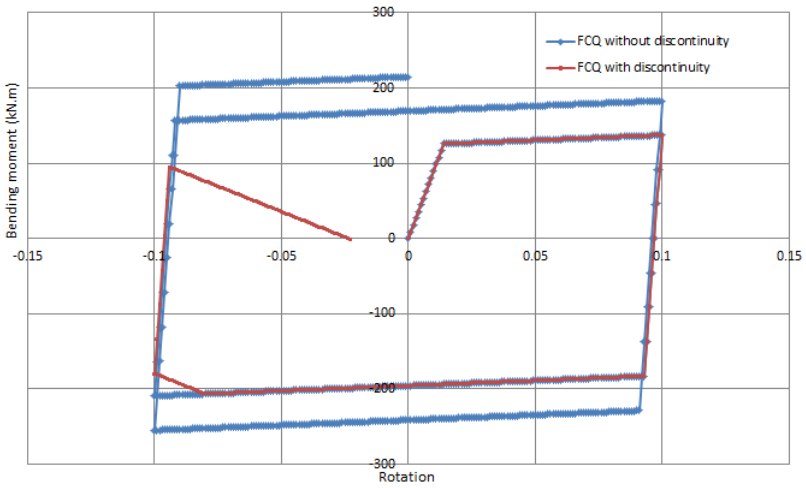

Figure 17: Cyclic response: FCQ formulation with and without embedded discontinuity

References

[1] Patrice Bailly. *Materials and Structures under Shock and Impact*. Wiley-ISTE, 2013.

[2] John M Biggs and Bernard Testa. *Introduction to structural dynamics*, volume 3. McGraw-Hill New York, 1964.

[3] Ibrahim Bitar, Stéphane Grange, Panagiotis Kotronis, and Nathan Benkemoun. A comparison of displacement-based Timoshenko multi-fiber beams finite element formulations and elasto-plastic applications. *European Journal of Environmental and Civil Engineering*, 22(4):464–490, 2018.

[4] Ibrahim Bitar, Panagiotis Kotronis, Nathan Benkemoun, and Stéphane Grange. A generalized Timoshenko beam with embedded rotation discontinuity. *Finite Elements in Analysis and Design*, 150:34–50, 2018.

[5] Marc Bonnet and Attilio Frangi. *Analyse des solides déformables par la méthode des éléments finis*. Editions de l'école polytechnique, 2007.

[6] Denis Caillerie, Panagiotis Kotronis, and Robert Cybulski. A Timoshenko finite element straight beam with internal degrees of freedom. *International Journal for Numerical and Analytical Methods in Geomechanics*, 39(16):1753–1773, 2015.

[7] Wensu Chen, Hong Hao, and Shuyang Chen. Numerical analysis of prestressed reinforced concrete beam subjected to blast loading. *Materials and Design*, 65:662–674, 2015.

[8] A R Dowling and J Harding. Tensile properties of mild steel under high strain rates. In *Proceedings of the 1st HERF Conf*, 1967.

[9] Hrvoje Draganić and Vladimir Sigmund. Blast Loading on Structures. *Technical Gazette*, 3:643–652, 2012.

[10] John Hetherington and Peter Smith. *Blast and ballistic loading of structures*. CRC Press, 2014.

[11] V. Karlos and G. Solomon. *Calculation of blast loads for application to structural components*. 2013.

[12] Gilbert F Kinney and Kenneth J Graham. *Explosive shocks in air*. Springer Science & Business Media, second edition, 2013.

[13] Jun Li and Hong Hao. Numerical study of concrete spall damage to blast loads. *International Journal of Impact Engineering*, 68:41–55, 2014.

[14] B. M. Luccioni, R. D. Ambrosini, and R. F. Danesi. Analysis of building collapse under blast loads. *Engineering Structures*, 26(1):63–71, 2004.

[15] T Ngo, P Mendis, M Hongwei, and S Mak. High strain rate behaviour of concrete cylinders subjected to uniaxial compressive impact loading. In *Proc. of 18th Australasian conference on the mechanics of structures and materials*, 2004.

[16] Joško Ožbolt, Akanshu Sharma, Baris Irhan, and Emiliano Sola. Tensile behavior of concrete under high loading rates. *International Journal of Impact Engineering*, 69:55–68, 2014.

[17] B. H. Pham, D. Brancherie, L. Davenne, and A. Ibrahimbegovic. Stress-resultant models for ultimate load design of reinforced concrete frames and multi-scale parameter estimates. *Computational Mechanics*, 51(3):347–360, 2013.

[18] U S Department of Defense. *UFC 3-340-02 Unified Facilities Criteria (UFC) Structures to resist the effects of accidental explosions.* 2008.

[19] Frank J Vecchio and Mohamed Basil Emara. Shear deformations in reinforced concrete frames. *ACI Structural journal*, 89(1):46–56, 1992.

[20] Bo Yan, Fei Liu, Dian Yi Song, and Zhi Gang Jiang. Numerical study on damage mechanism of RC beams under close-in blast loading. *Engineering Failure Analysis*, 51:9–19, 2015.